To cite this version :

Benjamin GUILLOT, Sébastien JEGOU, Laurent BARRALLIER - Influence of strain hardening on gaseous nitriding of steels - In: International Federation of Heat Treatment and Surface Engineering Congress 2016, 23rd IFHTSE Congress, Etats-Unis, 2016-04-18 - Conference Proceedings of the 23rd IFHTSE Congress - 2016

Influence of strain hardening on gaseous nitriding of steels

Benjamin GUILLOT, Dr. Sébastien JÉGOU, Prof. Laurent BARRALLIER
MSMP Laboratory, Arts&Métiers ParisTech, Aix-en-Provence, France.
benjamin.guillot@ensam.eu, sebastien.jegou@ensam.eu, laurent.barrallier@ensam.eu

Abstract

Machining is known to introduce plastic straining and residual stress gradients in surface of mechanical parts. If not controlled, the mechanical state of a surface can influence adsorption and diffusion of atoms during subsequent chemical surface treatments, such as nitriding. In the present work, the influence of strain hardening on gaseous nitriding of steels is studied. The nitriding process was carried out using a laboratory set-up enabling the control of nitriding parameters (time, temperature, nitriding potential) on 33CrMoV12-9 steel samples. Homogeneously strain hardened samples are obtained by controlled tensile tests, enabling to nitride samples at different levels of strengthening. Results are compared to a reference state, obtained from tensile specimen not submitted to strain-hardening, as well as an industrially representative sample nitrided using the same conditions. Nitrided samples are characterized by SEM observations, hardness measurements and carbon and nitrogen in-depth concentration profiles.

Introduction

Gaseous nitriding of steels plays a leading role over surface treatments in automotive and aeronautic industries.

Iron-based alloys involve catalytic decomposition of NH_3-rich atmosphere between 450 and 590 °C [1]. Diffusion of adsorbed nitrogen atoms can occur up to 1 mm in depth below the treated surface, depending on nitriding conditions (temperature T, time t, and nitriding potential K_N). The nitriding potential is defined as:

$$K_N = \frac{P_{NH_3}}{P_{H_2}^{3/2}}$$

where P_{NH3} and P_{H2} represents the partial pressures of ammonia and hydrogen respectively.

Nitrided surfaces are defined by a compound layer composed of ε-$Fe_{2-3}N$ and/or γ'-Fe_4N over a diffusion zone composed of finely dispersed alloying elements nitride MN (M= Cr, V, …) into a ferritic matrix with interstitially dissolved nitrogen and cementite at grain boundaries of prior austenite.

Influence of nitriding potential and temperature was described by Lehrer in the case of pure iron [2]. It results in surface strength hardening and the generation of compressive residual stresses ensuring a better resistance to fatigue and corrosion [3].

Gaseous nitriding is a very sensitive process and it is possible to fail nitriding while mastering nitriding parameters [4]. The phenomenon responsible for this prevention can be split in two categories: surface and bulk phenomenon.

The first category is known as catalytic deactivation and concerns the first few atomic layers, such as geometrical parameters (e.g. surface roughness) and surface chemical interaction (e.g. sulfur) [5]. The second group concerns mechanical interactions (residual stress and strain hardening) that can be induced by machining for example, and modifies microstructure up to hundredths of micrometers [6]. The following work only concerns the influence of strain hardening on nitriding. It is of great interest, as Tong showed that a strong defect density can significantly modify the thermodynamic stability of iron nitrides in the case of binary iron-based alloys, leading to the possible formation of a compound layer at low temperatures [7]. Kinetics of nitrides precipitation is generally enhanced by strain-hardening in the case of binary iron based-alloys [8-9]. From a more industrial point of view, it was shown that the presence of strong strain-hardening and surface recrystallization induced by cold burnishing of an AISI D2 tool steel before gaseous nitriding leads to a deeper diffusion of nitrogen and to higher microhardness values at considered depths [10]. However, the process of burnishing remains very restraining and could have a different influence on nitriding than a classical machining, like turning. The present work focuses on the influence of strain hardening on gaseous nitriding on an industrial steel grade 33CrMoV12-9 dedicated to nitriding.

Composition (wt.%)					
C	Cr	Mo	V	Mn	Fe
0.30	2.97	0.91	0.28	0.51	balance

Table 1: Chemical composition of the studied 33CrMoV12-9 steel grade.

Experimental details

Material parameter

The material used for the study is a 33CrMoV12-9 steel. It was austenitized at 920 °C for 90 min, quenched and tempered at 640 °C for 90 min under nitrogen atmosphere. The measured chemical composition of the alloy is detailed in Table 1. Chemical composition was obtained on several samples by spark emission spectroscopy.
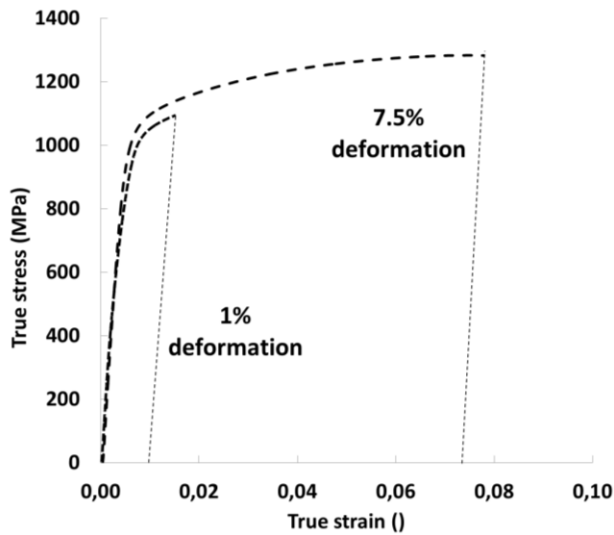
Figure 1: Tensile tests of 33CrMoV12-9 steel specimens stopped at different levels of strain hardening.

Strain hardening

Tensile specimens were carried out in order to study influence of strain hardening on the nitriding of steel. Specimens were wire and waterjet cut to an effective length of 60 mm. Strain hardening was obtained by tensile tests at two different levels of plastic deformation, 1 % and 7.5 %. No necking was observable after tensile testing of the samples.

Reference samples were taken from undeformed tensile specimen as well as samples that were submitted to industrial surface preparation, mainly based on milling, followed by grinding. These last samples were chosen as their microstructure is more representative of a structure industrially generated.

Specimens were cut in $18 \times 12 \times 5$ mm^3 parallelepipeds before nitriding.

Nitriding

Prior to nitriding, samples were grinded using a 1200-grit abrasive paper, followed by manual degreasing.

Gaseous nitriding was carried out in a Setsys Evolution thermogravimetric analyser from Setaram Instrumentation.

Before nitriding, a preliminary procedure based on vacuum and N_2 purges prevents samples from detrimental oxidation during the heating to the nitriding temperatures.

Nitriding was performed using a combination of NH_3, N_2 and H_2 at 520 °C with a $K_N = 3.7$ atm$^{-1/2}$ during 300 min (5 hours). The total gas flow rate of 200 ml.min^{-1} leads to a gas velocity of 10 mm.s^{-1}, ensuring a constant nitriding potential at the surface of the samples.

Heating and cooling of the samples were done at a rate of 10 °C.min^{-1}, under N_2 atmosphere.

During the treatment of samples, the dynamics of fluids might disturb the signal of the mass change. In order to remove any influence of the gas flow on the mass gain, a sample covered with copper, insensitive to ammonia decomposition was submitted to the same nitriding conditions. In data presented in Figure 2, the corresponding flux associated mass variation was subtracted to all experimental data, to only keep the nitriding associated mass variation.

Material analyses

Microstructure observations were carried out using a FEG-SEM JEOL JSM 7001F and backscattered electrons, with a 15 kV acceleration voltage. To this purpose, samples were grinded and polished down to 0.5 µm diamond solution, cleaned by ultrasounds during 5 min and etched with a 2%-nital solution.

Hardness measurements were carried out on a Leica VMHT device with a load of 2 N during 15 s.

Residual stress analysis was carried out by X-ray diffraction on a Siemens D500 diffractometer equipped with a linear detector and employing Cr-Kα radiation on the {211} diffracting plane of α-Fe. The sin²(Ψ) method was used to determine the residual stresses (σ_{xx}-σ_{zz}) in α-Fe.

Results

The stress-strain curves obtained by tensile testing are provided in Figure 1. The heat-treated material proved to have a yield stress of 1000 MPa, an ultimate stress of 1220 MPa, a maximum strain of about 15%, and a Young modulus of 212 GPa, which is coherent with standards. Both strain-hardening tests are consistent with the behavior law.

Several analyses of residual stress by X-ray diffraction at the surface of both tensile specimens before cutting were carried out, leading to a repetitive compressive residual stress of 150 MPa.

Thermogravimetric analysis

Mass gain profiles of nitrided samples are given in Figure 2.

The kinetics of mass gain vary during the first hours depending on the level of strain-hardening. The higher the strain-hardening, the faster the nitriding is. However, a steady state appears after nearly 150 min for all samples and the mass gain obtained after 5 h of nitriding are similar and close to 1.3 mg.cm^{-2}.

The unstrained reference sample shows a similar behavior to the low strain hardened sample, in terms on mass gain kinetics and final mass gain.

The sample obtained by industrial surface preparations shows a different behavior. The mass gain kinetics is higher during the first two hours. The final mass gain is close to 1.5 mg.cm^{-2}, which is more than all other samples. However, it also reaches a steady state after 200 min, leading to a constant mass gain of 0.16 mg.cm^{-2}.h^{-1} until the end of the treatment.
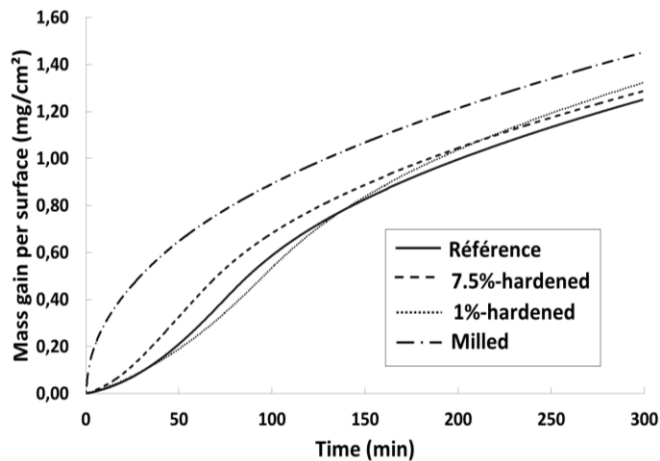
Figure 2: Mass gain of 33CrMoV12-9 steel specimen nitrided 5 h at 520 °C and 3.70 atm$^{-1/2}$

Microstructure observation

The comparison of the microstructure of strain-hardened samples shows that the nitrided depth is similar between all samples (Fig. 3). The compound layers are characterized by a thickness of about 10 μm.
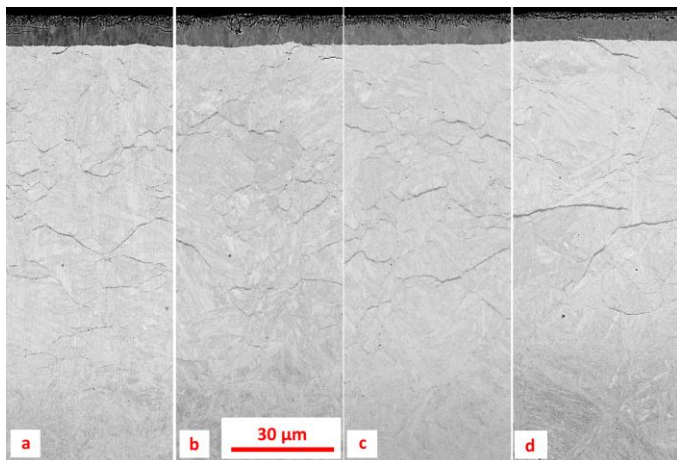

Figure 3: Scanning electron micrographs of nitrided 33CrMoV12-9 specimens. Comparison between the a) reference, b) 1% hardened, c) 7.5% hardened, and d) industrially prepared samples nitrided at 520 °C and 3.70 atm$^{-1/2}$ during 5 h.

Hardness profiles

Hardness profiles are given on Figure 4. They are all similar, including the milled sample. The bulk hardness is equal for all samples and reaches a value of 375 HV0.2. The effective depth, defined as the core hardness majored by 100 HV0.2, is equal to 140 μm for most samples, except the industrially prepared one, reaching an effective depth of 130 μm.
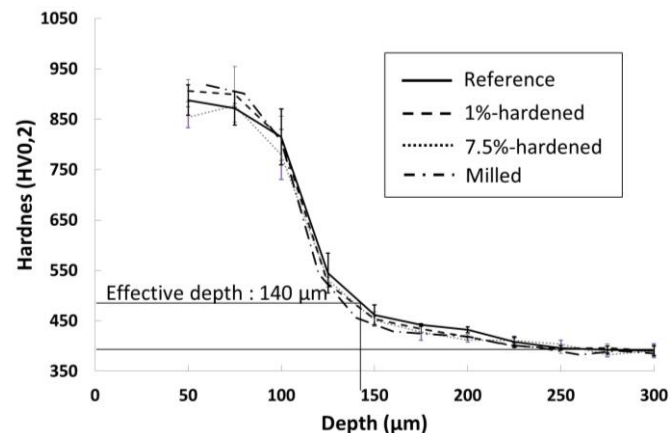

Figure 4: Hardness profiles of 33CrMoV12-9 specimens nitrided at 550 °C and 3.70 atm$^{-1/2}$ during 5 h.

Nitrogen and Carbon concentration

Nitrogen and carbon content in-depth profiles are given in Figure 5.
Surface measurements of nitrogen content cannot be provided due to a spectrometer measure limit of 1.3 wt.% exceeded by far in the compound layer.

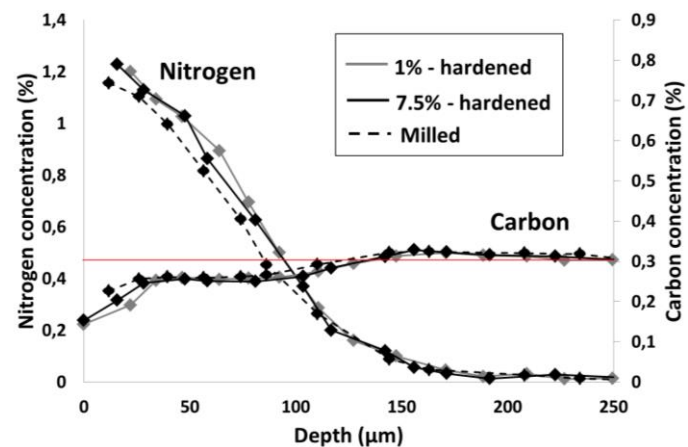Chemical content profiles are all similar and in agreement with hardness profiles and microstructure observation.

Figure 5: Carbon and nitrogen content in-depth profiles of strain-hardened samples nitrided at 520 °C and 3.70 atm$^{-1/2}$ during 5 h. The red horizontal line shows the carbon content of the base material (0.30 wt.%).

The enrichment of nitrogen close to the surface is not affected by the present strain-hardening from tensile test. The nitrogen concentration reaches null at 200 μm depth below the surface. Modification of the carbon content takes place up to 225 μm. Samples are also characterized by a carbon enrichment up to 0.34 wt.% at the nitrogen diffusion front, at 160 μm.

Discussion

Mass gain and loss

In the present work, the industrially prepared samples showed a faster nitriding kinetics and higher final mass gain. However, nitrogen and carbon content analyses of all samples indicate similar concentration gradients that results in no difference in hardness measurements.

In order to determine the origin of the final mass gain difference, one can calculate the mass gain and loss attributed to the diffusion layer by considering experimental nitrogen and carbon content profiles. A density of 7.8 mg.mm^{-3} was used in order to convert dimensions into mass.
For the carbon content, considering a bulk value of 0.30 wt.% and calculating the difference between measured and bulk values at each depth, a mass loss of approximately 0.39 mg.cm^{-2} for the whole sample is estimated.

For the mass gain of nitrogen in the diffusion layer, a null bulk concentration value is used for the calculation. This leads to a nitrogen mass gain of 0.85 mg.cm^{-2} in the diffusion layer from experimental nitrogen in-depth profiles.

The final mass gain associated with the diffusion layer is thus equal to 0.46 mg.cm^{-2}. According to the final mass gain obtained from experimental data, this leads to a calculated compound layer mass gain of 0.84 mg.cm^{-2} for the tensile specimens and 1.04 mg.cm^{-2} for the industrially prepared sample. It is then possible to calculate the theoretical thickness of the compound layer for different samples, estimating the mass gain of a compound layer, depending on its thickness.

It is known that the mass percentage of nitrogen in ε-Fe$_{2-3}$N and/or γ'-Fe$_4$N varies from 11 to 6 wt.%. Considering a linear decrease of the nitrogen content in the compound layer, which supposes an equal thickness of ε-Fe$_{2-3}$N and γ'-Fe$_4$N, the thickness of the compound layer is estimated as 12.7 µm for the tensile specimen and 15.7 µm for the industrially prepared sample.

It was not possible to validate these theoretical calculations by observations of the compound layer as the difference of thickness calculated is too small compared to the variation of the compound layer along the sample and the damages due to sample preparation.

However, considering the similar nitrogen and carbon content gradients, it can be concluded that the faster mass gain observed for the industrially prepared sample can then be attributed to a faster growth of the compound layer.

Theoretical influence of strain-hardening on nitriding

Strain-hardening of steels is expected to have two potentials effects on gaseous nitriding. The first effect concerns the impact of strain-hardening on nitrides formation.

Considering alloy composition for this study, nitrides formed are mainly Cr, Mo and V nitrides. Influence of defect density was studied by Selg on binary Fe-Mo alloy [11], for cold-rolled and recrystallized specimen. It was observed that nitriding kinetics is higher in the case of cold-rolled specimens. This was explained by the modification of nitrides precipitation by the high density of defects. In the case of recrystallized specimen, no Mo nitride precipitation was observed. As the solubility of Mo in the γ' layer is very low, its content in the ferritic matrix slows the formation of the compound layer, limiting the nitriding kinetics. However, in the case of cold-rolled specimen, the high-density of defects leads to the precipitation of hexagonal MoN and cubic Mo$_2$N. This precipitation leads to an easier formation of γ'-layer that overruns Mo nitrides instead of trying to form in a ferritic matrix, saturated with dissolved Mo.

In order to understand the influence of the density of defects on nitride precipitation, Biglari studied the nitriding of Fe-2wt.%Al samples obtained under different conditions, including cold-rolling and recrystallization [12]. The increase of the nitrogen content due to nitriding of recrystallized specimen leads to a precipitation of thermodynamically stable hexagonal, wurtzite type, AlN nitride. However, in the case of nitrided cold-rolled specimen, the presence of NaCl type AlN precipitates was observed.

The presence of such a thermodynamically unstable nitride was supposed to be possible due to the misfit conditions associated with their formation. The stable hexagonal nitride formation is associated with a large uptake of misfit-strain energy while precipitation of cubic AlN nitride is associated with a low increase of misfit-strain energy. Hexagonal and cubic nitride chemical Gibbs free energy of formation was estimated as -288 kJ.mol^{-1} and -69 kJ.mol^{-1}, respectively [12]. In the case of strain-hardened specimen, the presence of cubic AlN is possible if the increase of chemical Gibbs free energy associated with their formation is compensate with the decrease of misfit-strain energy of the matrix. It was also shown in different study that the content of aluminum strongly modifies the influence of strain-hardening [13].

In the present work, the mass gain kinetics increases with strain-hardening of tensile samples, which can be attributed to a faster precipitation of MoN and Mo$_2$N nitrides at the surface, due to a higher defect-density in the strain-hardened samples, leading to an easier formation of Fe$_4$N and a faster growth of compound layer. However, the levels of strain-hardening of the tensile specimen remain too low to observe a significant improve of nitrogen or carbon gradient, microstructure or mechanical properties of the diffusion layer. In most of the work studying influence of strain-hardening on nitriding, samples are cold-rolled to obtain a thickness reduction of 70 to 80% [12]. However, the strain-hardening of tensile samples is high enough in our work to have a non-meaningless improve of the mass gain kinetics.

In the case of the industrially prepared sample, the second potential expected effect of strain-hardening on nitriding, concerning surface recrystallization of the sample, should be considered. It is assumed that no recrystallization occurs for the tensile specimen, considering their low level of strain-hardening. However, for the industrially prepared sample, a recrystallization linked to surface milling can be expected, and could have a strong influence on nitriding kinetics. In the case of cathode sputtering before gaseous nitriding for example, which imposes strong lattice deformation at the surface of samples and strain-hardening, the process has proved to strongly increase the kinetics of white layer's nitride formation [14].

It should also be considered that tensile test is a monotonic test, while milling may impose cyclic plastic loadings to the sample and so, cumulative strains. Moreover, the mechanical loading in the case of milling induces more shearing. The higher mass gain kinetics of the milled sample tends to confirm such mechanical differences.

It should finally be considered that a single nitriding potential was used in this work. It may be assumed that the influence of a low strain-hardening would be more effective using a lower nitriding potential case. In order to verify this hypothesis, more experiments are planned, with the same levels of hardening, but lower nitriding potentials.

Conclusions

Influence of strain-hardening on gaseous nitriding of 33CrMoV12-9 steels has been studied. Two levels of strain-hardening were studied, 1 % and 7.5 % deformations, and compared to industrially representative samples. Such a level of hardening slightly modifies early mass gain kinetics but not the final mass gain, after 5 h of nitriding at 520°C. The faster kinetics is attributed to a faster growth of the compound layer due to a modification of nitride precipitation by strain hardening. However, it does not induce any differences in terms of neither microstructure, nor grain boundary precipitation, nor in terms of hardening. It appears that static loading tests are not well adapted for strain hardening study on gaseous nitriding of steels.

References

[1] Grabke, H.J., "Reaktionen von Ammoniak, Stickstoff und Wasserstoff and der Öberfläche von Eisen", Berichte der Bunsengesellchaft, Bd. 72, No. 4 (1968), pp. 533-541.

[2] Lehrer, E., "Uber das Eisen-Wasserstoff-Ammoniak-Gleichgewicht", vol. 36 (1930), pp. 383-392.

[3] Jack, D.H. *et al.*, "Effect of process variables on the fatigue resistance of nitrided steels", Heat treatment (1979), The Metal Society, pp. 169-177.

[4] Irretier, O. *et al.*, "Influence of contaminants on gas nitriding", Surface Engineering, vol. 12, No. 4 (1996), pp. 331-334.

[5] Arabczyk, W. *et al.*, "Poisoning of iron catalyst by sulfur", Catalysis Today, vol. 124 (2007), pp. 43-48.

[6] Haase, B. *et al.*, "Formation of reaction layers in steel machining: impact on surface treatment processes", Surface Engineering, vol. 15, No. 3 (1999), pp. 242-248.

[7] Tong, W.P., *et al.,* "Nitriding iron at lower temperatures", Science, vol. 299 (2003), pp. 686-686.

[8] Tong, W.P., *et al.*, "The formation of ε-$Fe_{2-3}N$ phase in a nanocrystalline Fe", Scripta Materialia, vol. 50 (2004), pp. 647-650.

[9] Brahmi, A. *et al.*, "Study of aluminum nitride precipitation in pure Fe-Al-N alloy by thermoelectric power measurement", Acta Materialia, vol. 45, No. 5 (1997), pp. 1889-1897.

[10] Tobola, D. *et al.*, "Structure and properties of burnished nitrided AISI D2 tool steel", Materials Science, vol. 21, No. 4 (2015), pp. 511-516.

[11] Selg, H. *et al.*, "Defect-dependant nitride surface layer development upon nitriding of Fe-1 at.% Mo alloy", Philosophical Magazine, vol. 93 (2013), pp. 2133-2160.

[12] Biglari, M.H. *et al.*, "Analysis of the nitrogen absorption isotherms of cold-rolled Fe-2 at.% Al specimens with different AlN precipitate dimensions", Philosophical magazine A, vol. 72, No. 4 (1995), pp. 931-947.

[13] Meka, S.R. *et al.*, "Interrelationships of defects, nitride modification and excess nitrogen"*,* International Journal of Materials research, vol. 105 (2014), pp. 1057-1066.

[14] Baranowska, J., "Influence of surface pretreatment on case formation during gaseous nitriding", Surface and Coatings Technology, vol. 125 (2000), pp. 30-34.